Inorg. Chem. **2006**, *45*, 767–778

Strong Electronic Interaction between Two Dimolybdenum Units Linked by a Tetraazatetracene

F. Albert Cotton,* Zhong Li, Chun Y. Liu, Carlos A. Murillo,* and Dino Villagrán

Department of Chemistry and Laboratory for Molecular Structure and Bonding, P.O. Box 3012, Texas A&M University, College Station, Texas 77842-3012

Received September 20, 2005

The large rigid dianion fluoflavinate, $C_{14}H_8N_4^{2-}$, consisting of four fused and planar six-membered rings with four nitrogen donor atoms, has been used to link two metal-to-metal bonded and redox-active Mo_2^{n+} units which are each locally bridged by three additional groups, collectively denoted [Mo_2]. In **1**, the [Mo_2] units are Mo_2(DAniF)$_3$ (DAniF = *N*,*N*′-di-*p*-anisylformamidinate), and in **5**, they are *trans*-Mo_2(DAniF)$_2$(O_2CCH_3) groups. These [Mo_2]-(fluoflavinate)[Mo_2] compounds show three reversible one-electron oxidation steps, one more than all other [Mo_2]-(linker)[Mo_2] species known to date. The first two redox processes are metal-based, and the third one has been assigned to a ligand oxidation by comparison to that of paddlewheel compound **4** which contains only one dimolybdenum unit with a monoanionic fluoflavinate ligand. Chemical oxidations of **1** produce the singly- and doubly-oxidized species **2** and **3**, respectively. All compounds have been characterized by X-ray crystallography and, as appropriate, by various techniques such as NMR, EPR, near-IR, and UV–vis. The fluoflavinate ligand strongly mediates electronic communication between the dimetal units, and the mixed valence species **2** can be described as electronically delocalized. Calculations at the DFT level using a variety of functionals support such an assignment and indicate that a strong transition in the NIR for the singly oxidized species can be assigned to the HOMO-1 to SOMO transition.

Introduction

Compounds with two redox sites, particularly those in which there are chemically identical metal-containing subunits, have been of interest since studies of the pyrazine-bridged diruthenium complex, the Creutz−Taube ion, began in the late 1960s.[1] In this compound, and in a large number of mixed valence (MV) analogues that have been synthesized since, the two metal centers are separated by a linker and there is an unpaired electron that may be distributed over the two metal units. In these MV compounds, the electronic communication or coupling between the units depends on the nature of the linker.[2,3] Therefore, the odd electron may stay on one end, move back and forth between the metal centers, or be equally distributed on both. A large number of experiments[4] and theoretical[5] efforts have been devoted to determine the factors that affect the strength of electronic coupling. Because understanding electron transfer within various components of a molecule is so important to many fields, the study of molecules of this type has increased considerably in the last several years. Many examples of MV species are found in the biological fields[6] and material sciences.[7] Because the conductive properties can be tuned by the bridging ligand, they can potentially be used as

* To whom correspondence should be addressed. E-mail: cotton@tamu.edu (F.A.C.); murillo@tamu.edu (C.A.M.).

(1) (a) Creutz, C.; Taube, H. *J. Am. Chem. Soc.* **1969**, *91*, 3988. (b) Creutz, C.; Taube, H. *J. Am. Chem. Soc*. **1973**, *95*, 1086.

(2) (a) Robin, M. B.; Day, P. *Adv. Inorg. Chem. Radiochem.* **1967**, *10*, 247. (b) Creutz. C. *Prog. Inorg. Chem.* **1983**, *30*, 1.

(3) There are also analogues with $Ru_3(\mu$-O) units. For example, see: (a) Ito, T.; Hamaguchi, T.; Nagino, H.; Yamaguchi, T.; Hirokaiki, K.; Zavarine, I. S.; Richmond, T.; Washington, J.; Kubiak, C. P. *J. Am. Chem. Soc*. **1999**, *121*, 4625. (b) Salsman, J. C.; Kubiak, C. P. *J. Am. Chem. Soc*. **2005**, *127*, 2382.

(4) (a) Richardson, D. E.; Taube, H. *Coord. Chem. Rev.* **1984**, *60*, 107. (b) Crutchley, R. J. *Adv. Inorg. Chem.* **1994**, *41*, 273. (c) Kaim, W.; Klein, A.; Glöckle, M. *Acc. Chem. Res.* **2000**, *33*, 755. (d) Demadis, K. D.; Harshorn, M.; Meyer, T. *J. Chem. Rev.* **2001**, *101*, 2655. (e) Nelsen, S. F. *Chem.—Eur. J*. **2000**, *6*, 581.

(5) (a) Sutin, N. *Prog. Inorg. Chem.* **1983**, *30*, 441. (b) Brunschwig, B. S.; Sutin, N. *Coord. Chem. Rev.* **1999**, *187*, 233. (c) Brunschwig, B. S.; Creutz, C.; Sutin, N. *Chem. Soc. Rev.* **2002**, *31*, 168.

(6) For example, see: (a) Blondin, G.; Gired, J.-J. *Chem. Rev*. **1990**, *90*, 1359 and references therein. (b) Gamelin, D. R.; Bominaar, E. L.; Kirk, M. L.; Wieghardt, K.; Solomon, E. I. *J. Am. Chem. Soc*. **1996**, *118*, 8085 and references therein.

(7) (a) Ward, M. D. *Chem. Soc. Rev.* **1995**, *34*, 121. (b) Astruc, D. *Acc. Chem. Res*. **1997**, *30*, 383. (c) McCleverty, J. A.; Ward, M. D. *Acc. Chem. Res*. **1998**, *31*, 842.

10.1021/ic051614d CCC: $33.50
Published on Web 12/06/2005

molecular wires, single-molecule transistors, or electronic components for a new generation of computers.[8] Undoubtedly, the study of MV compounds is expected to provide useful guidance for the development of metal−ligand hybrid material and molecular devices.

Recently, our group[9] and others[10] have been actively involved in studying MV compounds in which the two redox centers are composed of covalently bonded dimetal centers instead of the single-metal units previously used. There are at least two important advantages in employing certain dimetal centers as redox sites. Because the electronic properties of many dimetal units are well established, there is an unambiguous understanding of how the electronic structures (and thus the bond orders and metal-to-metal distances) of the dimetal units are affected by redox processes. For instance, for quadruply bonded M_2^{4+} units (M = Mo, W) the electronic configuration of $\sigma^2\pi^4\delta^2$ changes to $\sigma^2\pi^4\delta^1$ in the singly oxidized Mo_2^{5+} species.[11] The effect of a change in electronic structure can be monitored directly by the absorption from the $\delta \rightarrow \delta^*$ transitions and is also manifested very accurately in the metal−metal bond distances, which usually have very small esds.[12] While using the kinetically stable $[Mo_2(DAniF)_3]^+$ units (DAniF = *N*, *N*′-di-*p*-anisylformamidinate) as metal centers, we have structurally and spectroscopically characterized two systems that differ dramatically in the extent of the electron delocalization. In one system, $[Mo_2]^0M(OCH_3)_4[Mo_2]^{1+}$ (M = Zn, Co and $[Mo_2]$ represents the $[Mo_2(DAniF)_3]^+$ unit), the MV compounds are electronically localized,[13] but in the other, $[Mo_2]^{0.5+}$(β-oxamidate)$[Mo_2]^{0.5+}$, the system is delocalized.[14] Another important advantage of using dimetal units such as M_2^{4+} (M = Mo, W) instead of mononuclear units is that in such dimetal units the removal of an electron gives an electronic configuration in which there is certainty as to the shape of the orbital the unpaired electron occupies, namely a δ MO. In contrast, for metal atoms in mononuclear units there is often ambiguity about the type of SOMO because of low local symmetry[15] Thus, in compounds with dimetal units serving as redox sites, both experimental and theoretical studies can be conducted more efficiently, and the results are easier to interpret.

Scheme 1

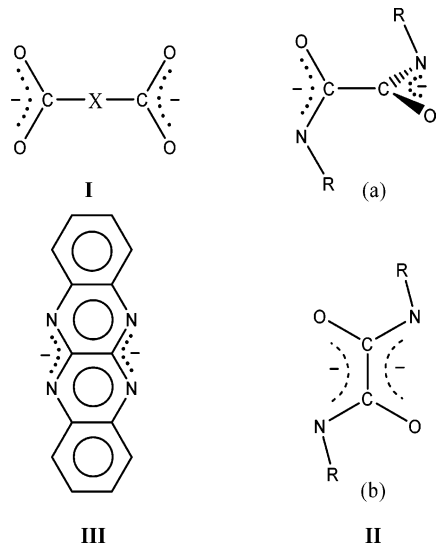

In our efforts to gain insight into the factors that lower the energy barrier and increase the electron-transfer rate, we have examined a wide variety of ligand functionalities including dicarboxylate anions ($O_2C-X-CO_2^{2-}$)[9a,b,c] with spacers, X (**I** in Scheme 1), of variable length and groups producing nonconjugated systems, such as tetrahedral ligands EO_4^{2-} (E = S, Mo, W)[9d] and $M(OCH_3)_4^{2-}$ (M = Zn, Co)[9e,13] that give compounds with two orthogonal dimetal units. The very basic diamidate ligands, **II**,[9f,14,16] have provided compounds with isomeric binding modes and conformations, **IIa** and **IIb**.

In the present work, the fluoflavinate anion (the dianion of 5,11-dihydroquinoxalino[2,3-*b*]quinoxaline, $C_{14}H_8N_4^{2-}$, **III**) is used to link two $[Mo_2]$ subunits. This linker features unusual structural, electronic, and chemical properties attributable to the rigidity of a large planar aromatic π system that extends throughout the four fused six-membered rings. This is the only all-nitrogen donor-linker that has so far been used to bind two dimetal centers. It should be noted that as the number of oxygen donor atoms diminishes by changing from dicarboxylate to fluoflavinate via diamidate groups, the basicity of the linkers significantly increases.

In contrast to all other dimolybdenum systems studied thus far that show a maximum of two redox waves, the $[Mo_2]$-(fluoflavinate)$[Mo_2]$ compound shows three reversible one-electron redox couples. Because of the "noninnocent" redox nature of the fluoflavinate linker, interesting questions are raised concerning the appearance of three, rather than only

(8) (a) Launary, J.-P. *Chem. Soc. Rev*. **2001**, *30*, 386. (b) Liang, W.; Shores, M. P.; Bockrath, M.; Long, J. R.; Park, H. *Nature* **2002**, *417*, 725.

(9) (a) Cotton, F. A.; Donahue, J. P.; Lin, C.; Murillo, C. A. *Inorg. Chem*. **2001**, *40*, 1234. (b) Cotton, F. A.; Donahue, P. J.; Murillo, C. A. *J. Am. Chem. Soc.* **2003**, *125*, 5436. (c) Cotton, F. A.; Donahue, P. J.; Murillo, C. A.; Pérez, L. M. *J. Am. Chem. Soc*. **2003**, *125*, 5486. (d) Cotton, F. A.; Donahue, J. P.; Murillo, C. A.; *Inorg. Chem*. **2001**, *40*, 2229. (e) Cotton, F. A.; Liu, C. Y.; Murillo, C. A.; Wang, X. *Inorg. Chem*. **2003**, *42*. 4619. (f) Cotton, F. A.; Daniels, L. M.; Donahue, J. P.; Liu, C. Y.; Murillo, C. A. *Inorg. Chem*. **2002**, *41*, 1354.

(10) (a) Bursten, B. E.; Chisholm, M. H.; Clark, R. J. H.; Firth, S.; Hadad, C.; Maclntosh, A. M.; Wilson, P. J.; Woodward, P. M.; Zaleski, J. M. *J. Am. Chem. Soc*. **2002**, *124*, 3050. (b) Bursten, B. E.; Chisholm, M. H.; Clark, R. J. H.; Firth, S.; Hadad, C.; Wilson, P. J.; Woodward, P. M.; Zaleski, J. M. *J. Am. Chem. Soc.* **2002**, *124*, 12244. (c) Bryrnes, M. J.; Chisholm, M. H.; Dye, D. F.; Hadad, C. M.; Pate, B. D.; Wilson, P. J.; Zaleski, J. M. *J. Chem. Soc., Dalton Trans.* **2004**, 523. (d) Chisholm, M. H. *Dalton Trans*. **2003**, 3821.

(11) Cotton, F. A., Murillo, C. A., Walton, R. A., Eds. *Multiple Bonds between Metal Atoms*, 3rd ed.; Springer Science and Business Media, Inc.: New York, 2005.

(12) (a) Cotton, F. A.; Hillard, E. A.; Murillo, C. A. *Inorg. Chem*. **2002**, *41*, 1639. (b) Cotton, F. A.; Daniels, L. M.; Murillo, C. A.; Wilkinson, C. C.; *J. Am. Chem. Soc*. **2002**, *124*, 9249. (c) Cotton, F. A.; Huang, P.; Murillo, C. A.; Timmons, D. J. *Inorg. Chem. Commun*. **2002**, *5*, 501.

(13) Cotton, F. A.; Dalal, N. S.; Liu, C. Y.; Murillo, C. A.; North, J. M.; Wang, X. *J. Am. Chem. Soc.* **2003**, *125*, 12945.

(14) Cotton, F. A.; Liu, C. Y.; Murillo, C. A.; Villagrán, D.; Wang, X. *J. Am. Chem. Soc*. **2004**, *126*, 14822.

(15) (a) Bunker, B. C.; Drago, R. S.; Hendrickson, D. N.; Richman, R. M.; Kessell, S. L. *J. Am. Chem. Soc.* **1978**, *100*, 3805. (b) Fürholz, U.; Burgi, H.-B.; Wagner, F. E.; Stebler, A.; Ammeter, J. H.; Krausz, E.; Clark, R. J. H.; Stead, M. J.; Ludi, A. *J. Am. Chem. Soc*. **1984**, *106*, 121. (c) Stebler, A.; Ammeter, J. H.; Fürholz, U.; Ludi, A. *Inorg. Chem*. **1984**, *23*, 2764.

two redox processes. To aid in the interpretation, three members of an electron-transfer series have been synthesized. These are the neutral compound, $[Mo_2(DAniF)_3]_2(C_{14}H_8N_4)$ (**1**), the mixed-valence ion, $\{[Mo_2(DAniF)_3]_2(C_{14}H_8N_4)\}^+$ in two crystalline forms (**2a** or **2b**), and the doubly oxidized cation, $\{[Mo_2(DAniF)_3]_2(C_{14}H_8N_4)\}^{2+}$ (**3**). Two additional compounds are also reported. One contains only one dimolybdenum unit with a monoanionic fluoflavinate ligand, $[Mo_2(DAniF)_3](HC_{14}H_8N_4)$ (**4**). The other one, **5**, is similar to **1** but it has *trans*-$Mo_2(DAniF)_2(O_2CCH_3)$ units instead of $Mo_2(DAniF)_3$. All compounds have been characterized using various techniques, including X-ray structure analyses, electrochemical measurements, and spectroscopic and magnetic studies that suggest that the MV species are electronically delocalized in the time scale of the experimental measurements. This conclusion is supported by the DFT calculations.

Experimental Section

Materials and Methods. All reactions and manipulations were performed under a nitrogen atmosphere, using either a nitrogen drybox or standard Schlenk line techniques. Solvents were purified under argon using a Glass Contour solvent purification system or distilled over appropriate drying agents under nitrogen. The starting materials, fluoflavine[17] and its 2-methyl derivative (5,12-dihydro-2-methylquinoxalino[2,3-*b*]quinoxaline),[17] $Mo_2(DAniF)_3(O_2CCH_3)$,[14] and *trans*-$Mo_2(DAniF)_2(O_2CCH_3)_2$[18] were prepared following reported procedures; commercially available chemicals were used as received.

Physical Measurements. Elemental analyses were performed by Canadian Microanalytical Service, Delta, British Columbia, Canada. Electronic spectra were measured on a Shimadzu UV-2501PC spectrometer in CH_2Cl_2 solution. ^{1}H NMR spectra were recorded on a Inova-300 NMR spectrometer with chemical shifts (δ) referenced to residual $CHCl_3$ in $CDCl_3$. Cyclic voltammograms and differential pulse voltammograms were collected on a CH Instruments electrochemical analyzer with Pt working and auxiliary electrodes, an Ag/AgCl reference electrode, a scan rate (for CV) of 100 mV/s, and 0.10 M Bu_4NPF_6 (in CH_2Cl_2) as the electrolyte. The near-IR spectrum was measured on a Bruker TEASOR 27 spectrometer using a KBr pellet. Magnetic susceptibility measurements were performed on a Quantum Design SQUID MPMS-XL magnetometer, and the EPR spectra were recorded using a Bruker ESP300 spectrometer.

Computational Details. Density functional theory (DFT)[19] calculations were performed with three different functionals. The hybrid functionals B3LYP[20] and mPW1PW91[21] and the gradient-corrected BP86[22] functional were used as implemented in the Gaussian 03 (revision C.02) program suite.[23] Double-ζ quality basis sets (D95)[24] were used on carbon, nitrogen, and hydrogen atoms. A small effective core potential (ECP) by Hay and Wadt, representing the 1s2s2p3s3p3d core was used for the molybdenum atoms, along with its corresponding double-ζ basis set (LANL2DZ).[25] TD-DFT[26] calculations were performed to ascertain the identity of the lowest-energy transitions in the UV−vis and NIR regions for **1** and **2**. All calculations were performed on either an Origin 3800 64-processor SGI, an Origin 2000 32-processor SGI computer located at the Texas A&M supercomputing facility, or an Origin 300 8-processor SGI located at the Department of Chemistry at Texas A&M University.

Preparation of $[Mo_2(DAniF)_3]_2(C_{14}H_8N_4)$, 1. Two milliliters of a 0.5 M solution of $NaOCH_3$ in methanol was added slowly with stirring to a mixture of $Mo_2(DAniF)_3(O_2CCH_3)$ (812 mg, 0.800 mmol) and fluoflavine (94 mg, 0.40 mmol) in 40 mL of THF. The yellow solution turned orange and then dark brown. The reaction mixture was stirred overnight at ambient temperature. The solvent was removed under reduced pressure, and the residue was extracted with 15 mL of dichloromethane. After filtration, the volume of the solution was reduced under vacuum to ca. 5 mL. Ethanol (50 mL) was added to the solution, and an orange precipitate formed. The supernatant solution was decanted, and the solid was washed with ethanol (2 × 15 mL), followed by hexanes (2 × 15 mL). The solid was dissolved in 15 mL of dichloromethane, and the solution was layered with hexanes. Orange needle crystals formed in 5 days. Yield: 580 mg (68%). ^{1}H NMR ($CDCl_3$): δ 8.65 (s, 2H, −NC*H*N−), 8.323 (s, 4H, −NC*H*N−), 6.62 (d, 8H, aromatic C−*H*), 6.54 (d, 16H, aromatic C−*H*), 6.50 (d, 16H, aromatic C−*H*), 6.27 (d, 8H, aromatic C−*H*), 5.69 (m, 4H, fluoflavinate C−*H*), 3.78 (s, 12H, −CH_3), 3.69 (s, 24H, −CH_3), 3.52 (m, 4H, fluoflavinate C−*H*). UV−vis, λ_{max} (ϵ): 412 (2.4×10^3), 432 (3.0×10^2), 460 (8.0×10^2), 482 (2.0×10^2), 512 nm (1.0×10^3 M^{-1} mol^{-1}). Anal. Calcd for $C_{104}H_{98}Mo_4N_{16}O_{12}$: C, 58.15; H, 4.57; N, 10.43. Found: C, 58.53; H, 4.67; N, 10.38.

Preparation of $\{[Mo_2(DAniF)_3]_2(C_{14}H_8N_4)\}PF_6$, 2a. Solutions of **1** (215 mg, 0.100 mmol in 10 mL of CH_2Cl_2) and ferrocenium hexafluorophosphate (36 mg, 0.11 mmol in 10 mL of CH_2Cl_2) were prepared separately and cooled to −78 °C. The Cp_2FePF_6 solution was added to the solution of **1**, and the mixture turned dark brown immediately. The mixture was allowed to warm to room temperature with stirring over the course of 1 h. Then, hexanes (40 mL) were added to precipitate a very dark brown solid. After the yellow supernatant solution was decanted, the solid was washed with

(16) Cotton, F. A.; Liu, C. Y.; Murillo, C. A.; Villagrán, D.; Wang, X. *J. Am. Chem. Soc.* **2003**, *125*, 13564.
(17) Fisher, H. M.; Lusi, A.; Egerton, R. J. *J. Pharm. Sci.* **1977**, *66*, 1349.
(18) Cotton, F. A.; Liu, C. Y.; Murillo, C. A. *Inorg. Chem.* **2004**, *43*, 2267.
(19) (a) Hohenberg, P.; Kohn, W. *Phys. Rev.* **1964**, *136*, B864. (b) Parr, R. G.; Yang, W. *Density-Functional Theory of Atoms and Molecules*; Oxford University Press: Oxford, U.K., 1989.
(20) (a) Becke, A. D. *Phys. Rev. A* **1988**, *38*, 3098. (b) Becke, A. D. *J. Chem. Phys.* **1993**, *98*, 1372. (c) Becke, A. D. *J. Chem. Phys.* **1993**, *98*, 5648. (c) Lee, C.; Yang, W.; Parr, R. G. *Phys. Rev. B* **1988**, *37*, 785.
(21) Adamo, C.; Barone, V. *J. Chem. Phys.* **1998**, *108*, 664.
(22) (a) Becke, A. D. *Phys. Rev. A* **1988**, *38*, 3098. (b) Perdew, J. P. *Phys. Rev. B* **1986**, *33*, 8822.
(23) Frisch, M. J.; Trucks, G. W.; Schlegel, H. B.; Scuseria, G. E.; Robb, M. A.; Cheeseman, J. R.; Montgomery, J. A., Jr.; Vreven, T.; Kudin, K. N.; Burant, J. C.; Millam, J. M.; Iyengar, S. S.; Tomasi, J.; Barone, V.; Mennucci, B.; Cossi, M.; Scalmani, G.; Rega, N.; Petersson, G. A.; Nakatsuji, H.; Hada, M.; Ehara, M.; Toyota, K.; Fukuda, R.; Hasegawa, J.; Ishida, M.; Nakajima, T.; Honda, Y.; Kitao, O.; Nakai, H.; Klene, M.; Li, X.; Knox, J. E.; Hratchian, H. P.; Cross, J. B.; Bakken, V.; Adamo, C.; Jaramillo, J.; Gomperts, R.; Stratmann, R. E.; Yazyev, O.; Austin, A. J.; Cammi, R.; Pomelli, C.; Ochterski, J. W.; Ayala, P. Y.; Morokuma, K.; Voth, G. A.; Salvador, P.; Dannenberg, J. J.; Zakrzewski, V. G.; Dapprich, S.; Daniels, A. D.; Strain, M. C.; Farkas, O.; Malick, D. K.; Rabuck, A. D.; Raghavachari, K.; Foresman, J. B.; Ortiz, J. V.; Cui, Q.; Baboul, A. G.; Clifford, S.; Cioslowski, J.; Stefanov, B. B.; Liu, G.; Liashenko, A.; Piskorz, P.; Komaromi, I.; Martin, R. L.; Fox, D. J.; Keith, T.; Al-Laham, M. A.; Peng, C. Y.; Nanayakkara, A.; Challacombe, M.; Gill, P. M. W.; Johnson, B.; Chen, W.; Wong, M. W.; Gonzalez, C.; Pople, J. A. *Gaussian 03*, revision C.02; Gaussian, Inc.: Wallingford, CT, 2004.
(24) (a) Dunning, T. H.; Hay, P. J. In *Modern Theoretical Chemistry. 3. Methods of Electronic Structure Theory*; Schaefer, H. F., III, Ed.; Plenum Press: New York, 1977; pp 1−28. (b) Woon, D. E.; Dunning, T. H. *J. Chem. Phys.* **1993**, *98*, 1358.
(25) (a) Wadt, W. R.; Hay, P. J. *J. Chem. Phys.* **1985**, *82*, 284. (b) Hay, P. J.; Wadt, W. R. *J. Chem. Phys.* **1985**, *82*, 299.
(26) Casida, M. E.; Jamorski, C.; Casida, K. C.; Salahub, D. R. *J. Chem. Phys.* **1998**, *108*, 4439.

hexanes (2 × 15 mL) and dried under vacuum. The dry solid was dissolved in 15 mL of dichloromethane, and the solution was layered with hexanes. Large block-crystals formed in 3 days. Yield: 190 mg (83.0%). UV−vis, λ_{max} (ϵ): 420 (2.2×10^3), 454 (3.0×10^2), 550 (2.0×10^3), 622 nm (3.0×10^2 M^{-1} mol^{-1}). Anal. Calcd for $C_{104}H_{98}PF_6Mo_4N_{16}O_{12}$: C, 54.50; H, 4.28; N, 9.77. Found: C, 54.83; H, 4.12; N, 9.89.

Preparation of {[Mo$_2$(DAniF)$_3$]$_2$(C$_{14}$H$_8$N$_4$)}SO$_3$CF$_3$, 2b. Solutions of **1** (107 mg, 0.050 mmol in 10 mL of CH_2Cl_2) and $AgSO_3CF_3$ (13 mg, 0.050 mmol in 10 mL of CH_2Cl_2) were prepared separately and cooled to −78 °C. The $AgSO_3CF_3$ solution was added to the solution of **1**, and the mixture turned very dark brown immediately. The mixture was allowed to warm to ambient temperature with stirring over the course of 1 h and was then filtered through a filter frit packed with Celite. The filtrate was layered with hexanes, and black crystals formed in 3 days. Yield: 60 mg (53%). UV−vis, λ_{max} (ϵ): 410 (1.0×10^2), 436 (1.3×10^3), 454 (2.0×10^2), 550 (1.3×10^3), 620 nm (1.6×10^2 M^{-1} mol^{-1}).

Preparation of {[Mo$_2$(DAniF)$_3$]$_2$(C$_{14}$H$_8$N$_4$)}(PF$_6$)$_2$, 3. Solutions of **1** (274 mg, 0.128 mmol in 10 mL of CH_2Cl_2) and $AgPF_6$ (65 mg, 0.26 mmol in 20 mL of CH_2Cl_2) were prepared separately and cooled to −78 °C. The $AgPF_6$ solution was added to the solution of **1**, and the mixture became black immediately. The mixture was allowed to warm to room temperature with stirring over the course of 1 h and was then filtered through a filter frit packed with Celite. The filtrate was layered with hexanes, and black crystals formed in 3 days. Yield: 80 mg (33%). Anal. Calcd for $C_{105}H_{100}P_2F_{12}Mo_4N_{16}O_{12}Cl_2$ (**3**·CH_2Cl_2): C, 49.98; H, 3.97; N, 8.89. Found: C, 49.91; H, 4.26; N, 8.54. UV−vis, λ_{max} (ϵ): 434 (1.2×10^3), 462 (3.3×10^2), 548 (4.7×10^2), 636 nm (1.1×10^2 M^{-1} mol^{-1}).

Preparation of Mo$_2$(DAniF)$_3$(HC$_{14}$H$_8$N$_4$), 4. THF (30 mL) was added to a mixture of $Mo_2(DAniF)_3(O_2CCH_3)$ (203 mg, 0.200 mmol) and fluoflavine (55 mg, 0.23 mmol) giving a yellow suspension. Two milliliters of a 0.5 M solution of $NaOCH_3$ in methanol was added slowly with stirring, and the reaction mixture was stirred overnight at ambient temperature. After the solvent was removed under reduced pressure, the yellow residue was extracted with 15 mL of dichloromethane and filtered through a Celite-packed frit. Ethanol (ca. 40 mL) was added to the filtrate yielding a yellow solid. After the supernatant solution was decanted, the solid was washed with 15 mL of hexanes and then redissolved in 10 mL of dichloromethane. The resulting solution was then layered with 40 mL of hexanes. Orange needle crystals formed in 5 days. Yield: 80 mg (36%). ^{1}H NMR ($CDCl_3$): δ 8.60 (s, 1H, −NC*H*N−), 8.20 (s, 2H, −NC*H*N−), 6.70 (d, 2H, fluoflavinate C−*H*), 6.61 (d, 4H, aromatic C−*H*), 6.56 (t, 2H, fluoflavinate C−*H*), 6.45 (s, 16H, aromatic C−*H*), 6.24 (d, 4H, aromatic C−*H*), 6.96 (t, 2H, fluoflavinate C−*H*), 3.74 (s, 6H, −C*H*$_3$), 3.65 (s, 12H, −C*H*$_3$), 3.62 (t, 2H, fluoflavinate C−*H*). UV−vis, λ_{max} (ϵ): 410 (2.3×10^3), 451 (1.2×10^3), 512 nm (6.0×10^2 M^{-1} mol^{-1}).

Preparation of [*trans*-Mo$_2$(DAniF)$_2$(O$_2$CCH$_3$)]$_2$(C$_{14}$H$_8$N$_4$), 5. A suspension of fluoflavine (47 mg, 0.20 mmol) in 15 mL of THF was cooled to −20 °C, and 0.25 mL of a 1.6 M methyllithium solution in diethyl ether was added. The suspension of lithium fluoflavinate salt that formed upon warming the mixture to room temperature was transferred to a flask containing a solution of *trans*-$Mo_2(DAniF)_2(O_2CCH_3)_2$ (328 mg, 0.400 mmol) in 15 mL of THF. The reaction mixture was stirred overnight, and an orange precipitate formed. After the solvent was removed under reduced pressure, 20 mL of dichloromethane was added to the orange residue, and the resulting solution was filtered. The volume of the filtrate was reduced to about 5 mL under vacuum, and 40 mL of hexanes were added to precipitate an orange solid. After the solvent was decanted, the solid was washed with ethanol (2 × 15 mL) and hexanes (2 × 15 mL) and dried under vacuum. The solid was dissolved in 15 mL of dichloromethane, and the solution was then layered with hexanes. Orange crystals formed in 2 days. Yield: 90 mg (26%) ^{1}H NMR ($CDCl_3$): δ 8.45 (s, 4H, −NC*H*N−), 6.80 (d, 16H, aromatic C−*H*), 6.66 (d, 16H, aromatic C−*H*), 5.68 (m, 4H, aromatic C−*H*), 3.71 (s, 24H, −C*H*$_3$), 3.62 (m, 4H, aromatic C−*H*), 2.75 (s, 6H, −O_2CC*H*$_3$). UV−vis, λ_{max} (ϵ): 412 (2.5×10^3), 446 (9.0×10^2), 482 (1.0×10^2), 514 nm (2.4×10^2 M^{-1} mol^{-1}). Anal. Calcd for $C_{82}H_{78}Mo_4N_{12}O_{12}Cl_8$ (**5**·$4CH_2Cl_2$): C, 47.06 H, 3.90; N, 8.36. Found: C, 47.01; H, 3.97; N, 8.09.

X-ray Structure Determinations. Crystals of **1**·$4CH_2Cl_2$, **2b**·$7.5CH_2Cl_2$, **3**·$4CH_2Cl_2$, **4**, and **5**·$4CH_2Cl_2$ suitable for X-ray analyses were prepared by diffusion of hexanes into the corresponding dichloromethane solutions. Each crystal was mounted and centered in the goniometer of a Bruker SMART 1000 CCD area detector diffractometer and cooled to −60 °C. Cell parameters were determined using the program SMART.[27] Data reduction and integration were performed with the software package SAINT,[28] while absorption corrections were applied using the program SADABS.[29] In all structures, the positions of the heavy atoms were found via direct methods using the program SHELXTL.[30] Subsequent cycles of least-squares refinement followed by difference Fourier syntheses revealed the positions of the remaining non-hydrogen atoms. Hydrogen atoms were added in idealized positions. Non-hydrogen atoms were refined with anisotropic displacement parameters. Some of the anisyl group in the DAniF ligands and interstitial CH_2Cl_2 molecules were found to be disordered, and they were refined with soft constraints. Crystallographic data for **1**·$4CH_2Cl_2$, **2b**·$7.5CH_2Cl_2$, **3**·$4CH_2Cl_2$, **4**, and **5**·$4CH_2Cl_2$ are listed in Table 1, and selected bond distances for these compounds are given in Table 2.

Results and Discussion

Synthesis. In prior work, we developed two general procedures for the preparation of the "dimer-of-dimers" type molecules, which may be described by the general formula $[Mo_2(DAniF)_3]L[Mo_2(DAniF)_3]$, where L represents a linker. The source of dimolybdenum units can be either the $[Mo_2(DAniF)_3(NCCH_3)_2]^+$ cation[9a,31] or $Mo_2(DAniF)_3(O_2CCH_3)$,[14] the choice of which depends on the basicity of the linker. For example, when the linker is a strong Lewis base which may nucleophilically attack the coordinated acetonitrile molecules, $Mo_2(DAniF)_3(O_2CCH_3)$ is the appropriate starting material.[9f,14] For the very weak acid fluoflavine ($H_2C_{14}H_8N_4$), the conjugate base ($C_{14}H_8N_4^{2-}$) is a strong Lewis base, and therefore, $Mo_2(DAniF)_3(O_2CCH_3)$, rather than $[Mo_2(DAniF)_3(NCCH_3)_2]^{2+}$, was used in the synthesis of $[Mo_2(DAniF)_3]_2(C_{14}H_8N_4)$. The overall reaction that led to synthesis of **1** is

$$2Mo_2(DAniF)_3(O_2CCH_3) + H_2(C_{14}H_8N_4) + 2NaOCH_3 \rightarrow [Mo_2(DAniF)_3]_2(C_{14}H_8N_4) + 2CH_3OH + 2NaO_2CCH_3$$

(27) *SMART*, version 5.05; Bruker Analytical X-ray System, Inc.: Madison, WI, 1998.
(28) *SAINT. Data Reduction Software*, version 6.36A; Bruker Analytical X-ray System, Inc.: Madison, WI, 2002.
(29) *SADABS. Bruker/Siemens Area Detector Absorption and Other Corrections*, version 2.03; Bruker Analytical X-ray System, Inc.: Madison, WI, 2002.
(30) Sheldrick, G. M, *SHELXTL*, version 6.12; Bruker Analytical X-ray Systems, Inc.: Madison, WI, 2000.

Table 1. X-ray Crystallographic Data for **1**, **2b**, **3**, **4**, and **5**

	1·4CH_2Cl_2	**2b**·7.5CH_2Cl_2	**3**·4CH_2Cl_2
empirical formula	$C_{108}H_{106}Cl_8Mo_4N_{16}O_{12}$	$C_{112.5}H_{113}Cl_{15}F_3Mo_4N_{16}O_{15}S$	$C_{108}H_{106}Cl_8F_{12}Mo_4N_{16}O_{12}P_2$
fw	2487.45	2933.76	2777.39
space group	$P\bar{1}$ (No. 2)	$P2_1/n$ (No. 14)	$P\bar{1}$ (No. 2)
a (Å)	12.3728(8)	17.881(5)	12.336(1)
b (Å)	15.864(1)	23.811(6)	16.948(2)
c (Å)	15.948(1)	29.914(8)	17.203(2)
α (deg)	60.320(1)	90	60.865(2)
β (deg)	89.858(1)	93.715(5)	81.414(2)
γ (deg)	84.897(1)	90	70.215(2)
V (Å^3)	2705.9(3)	12710(6)	2955.7(6)
Z	1	4	1
T (K)	213	213	213
λ (Å)	0.71073	0.71073	0.71073
d_{calcd} (g/cm^3)	1.526	1.533	1.560
μ (mm^{-1})	0.718	0.787	0.706
R1[a] (wR2[b])	0.0463 (0.1043)	0.0937 (0.1786)	0.0626 (0.1069)

	4	**5**·4CH_2Cl_2
empirical formula	$C_{59}H_{54}Mo_2N_{10}O_6$	$C_{82}H_{82}Cl_8Mo_4N_{12}O_{12}$
fw	1191.00	2094.96
space group	$P2_1/c$ (No.14)	$P\bar{1}$ (No. 2)
a (Å)	14.6700(9)	10.533(2)
b (Å)	17.894(1)	14.862(3)
c (Å)	20.725(1)	15.070(3)
α (deg)	90	89.761(4)
β (deg)	95.358(1)	73.296(4)
γ (deg)	90	75.536(4)
V (Å^3)	5416.9(6)	2182.0(9)
Z	4	1
T (K)	213	213
λ (Å)	0.71073	0.71073
d_{calcd} (g/cm^3)	1.460	1.594
μ (mm^{-1})	0.525	0.873
R1[a] (wR2[b])	0.0426 (0.0888)	0.0922 (0.1653)

[a] $R1 = \sum||F_o| - |F_c||/\sum|F_o|$. [b] $wR2 = [\sum[w(F_o^2 - F_c^2)^2]/\sum[w(F_o^2)^2]]^{1/2}$.

Table 2. Selected Bond Lengths (Å) for **1**, **2b**, **3**, **4**, and **5**

	1·4CH_2Cl_2	**2b**·7.5CH_2Cl_2	**3**·4CH_2Cl_2	**4**	**5**·4CH_2Cl_2
Mo(1)−Mo(2)	2.0939(4)	2.1084(8)	2.1245(5)	2.0931(3)	2.0818(8)
Mo(3)−Mo(4)		2.1108(8)			
Mo(1)−N(1)	2.156(3)	2.132(5)	2.143(3)	2.171(2)	2.137(5)
Mo(1)−N(3)	2.161(3)	2.132(5)	2.144(3)	2.155(2)	2.141(5)
Mo(1)−N(5)	2.162(3)	2.150(5)	2.128(3)	2.149(2)	
Mo(1)−O(5)					2.132(4)
Mo(1)−N(7)	2.160(3)	2.150(5)	2.111(3)	2.154(2)	2.146(5)
Mo(2)−N(2)	2.169(3)	2.129(5)	2.117(3)	2.144(2)	2.133(5)
Mo(2)−N(4)	2.150(3)	2.144(5)	2.109(3)	2.152(2)	2.138(5)
Mo(2)−N(6)	2.161(3)	2.135(5)	2.117(3)	2.160(2)	
Mo(2)−O(6)					2.139(5)
Mo(2)−N(8)	2.135(3)	2.129(5)	2.137(3)	2.159(2)	2.164(5)
Mo(3)−N(9)		2.128(5)			
Mo(3)−N(11)		2.148(5)			
Mo(3)−N(13)		2.137(5)			
Mo(3)−N(15)		2.136(5)			
Mo(4)−N(10)		2.122(5)			
Mo(4)−N(12)		2.142(5)			
Mo(4)−N(14)		2.154(5)			
Mo(4)−N(16)		2.132(5)			

Compound **1** is soluble in common organic solvents, such as tetrahydrofuran and dichloromethane, even though fluoflavine is highly insoluble in these solvents. After routine treatment, the reaction produces crystalline material in a useful yield.

It should be noted that the above-mentioned equation does not mechanistically reflect what actually occurs during the reaction because we have found that, in methanol, $NaOCH_3$ reacts readily with $Mo_2(DAniF)_3(O_2CCH_3)$ yielding a stable compound $Mo_2(DAniF)_3(OCH_3)(CH_3OH)$,[32] and this is a likely intermediate in the reaction. When a ligand H_2L such as fluoflavine has a pK_a close to or larger than that of CH_3OH (15.5), it is possible that $Mo_2(DAniF)_3(OCH_3)(CH_3OH)$ forms first and, following self-assembly with the H_2L ligand, results in the desired dimer-of-dimers product.

The chemical oxidation of **1** was guided by electrochemical data. The cyclic voltammogram (CV) and differential pulse voltammogram (DPV) (Figure 1) show three reversible redox waves. This contrasts with all known $[Mo_2]L[Mo_2]$ analogues, such as those with dicarboxylate and diamidate linkers in which only two waves were observed. The three successive one-electron oxidations occur at potentials of 79, 495, 941 mV (vs Ag/AgCl). Ferrocenium hexafluorophosphate was chosen to remove one electron from the neutral molecule **1**, and the stronger oxidant $AgPF_6$ was used for the synthesis of the doubly oxidized cation. The advantage of using Cp_2FePF_6 for the preparation of the monocharged complex is that the reaction gives **2a** in high yield without contamination by the doubly oxidized species, even when the oxidizing reagent is present in excess. However, when silver trifluoromethanesulfonate was used for the preparation of the singly oxidized complex **2b**, it was very important to

(31) Chisholm, M. H.; Cotton, F. A.; Daniels, L. M.; Folting, K.; Huffman, J. C.; Iyer, S. S.; Lin, C.; MacIntosh, A. M.; Murillo, C. M. *J. Chem. Soc., Dalton Trans.* **1999**, 1387.

(32) Cotton, F. A.; Liu, C. Y.; Murillo, C. A. Unpublished results.

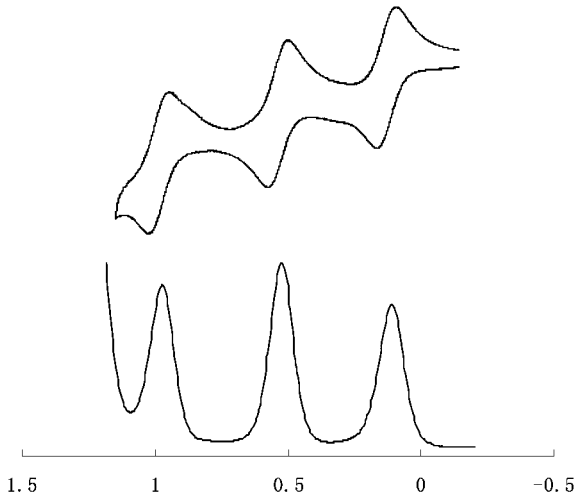

Figure 1. Cyclic voltammogram and differential pulse voltammogram (DPV) for **1** in CH_2Cl_2 solution (with potentials vs Ag/AgCl).

carefully control the reaction stoichiometry to avoid further oxidation.

The dication in **3** was prepared using $AgPF_6$ as the oxidizing agent. In practice, more than 2 equiv of the oxidizing reagent must be used to obtain a product of acceptable purity for elemental analysis. This compound is not stable in solution at ambient temperature, and even in the solid state, there are signs of decomposition after a few hours.

It is clear from the electrochemistry that the third oxidation of **1** would require a very strong oxidizing reagent, and all attempts to isolate such highly charged species have so far been unsuccessful.

The paddlewheel compound, $Mo_2(DAniF)_3(HC_{14}H_8N_4)$, **4**, was prepared using a modification of the procedure described above for **1**. The strategy used to avoid the possibility of obtaining the dimer-of-dimers was to control the amount of the methoxide base. The ratio of base to Mo_2 species was 1:1 to form the intermediate $Mo_2(DAniF)_3(OCH_3)(CH_3OH)$ but fluoflavine was used in excess. Because in **4** the free N−C−N group of the fluoflavinate ligand is protonated, it is capable of binding another $[Mo_2]$ unit if additional base were to be added. Such molecules are usually active or unstable, and formation of $[Mo_2]L[Mo_2]$ species may occur even in the absence of strong base. For example, a reaction of dicarboxylic acid with $Mo_2(DAniF)_3(O_2CCH_3)$ produces only $[Mo_2]$(dicarboxylate])$[Mo_2]$ compounds, regardless of the stoichiometry of the reactants added. An amidate analogue of **2** has been isolated, but it immediately dimerizes in basic solution.[32] Interestingly, **2** is stable, and there is no evidence of dimerization occurring in solution. The unusual stability of **2** may be attributed to the very weak acidity of the fluoflavine ligand.

Compound **5** may be viewed as a derivative of **1** by replacement of one DAniF group on each $[Mo_2]$ unit with an acetate anion. It was prepared in a one-pot reaction by mixing *trans*-$Mo(DAniF)_2(O_2CCH_3)_2$ with lithium fluoflavinate. The doubly deprotonated ligand displaces only one acetate group from each of two *trans*-$Mo(DAniF)_2(O_2CCH_3)_2$ molecules, giving **5**. It is plausible that since the precursor

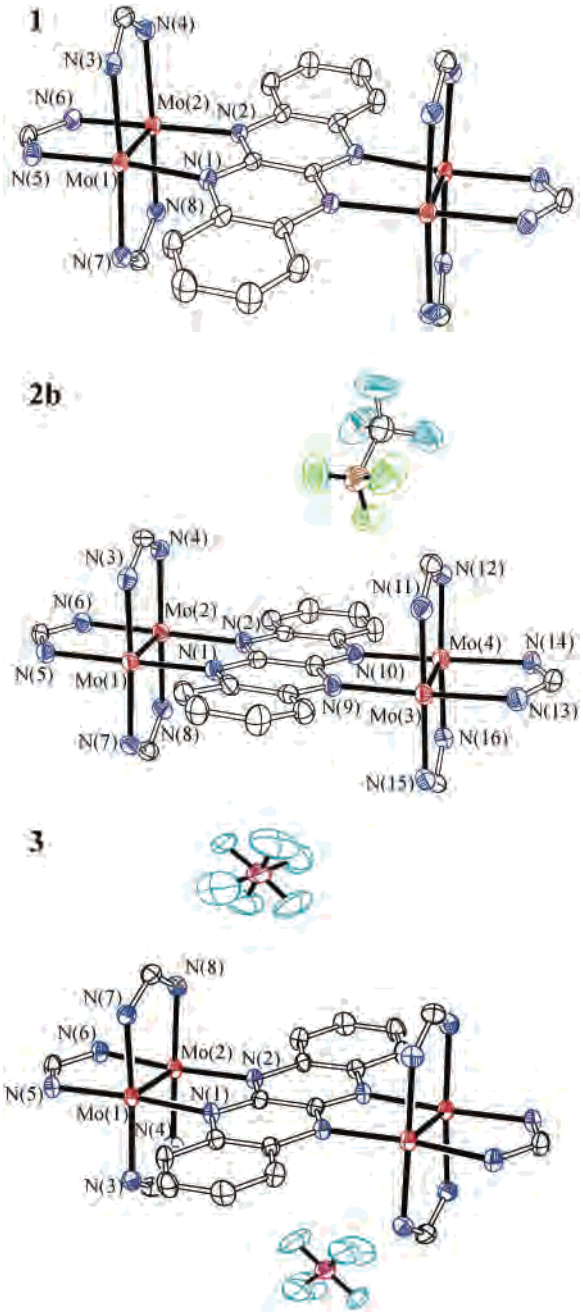

Figure 2. Core of **1**, **2b**, and **3** with displacement ellipsoids drawn at the 40% probability level. All *p*-anisyl groups and hydrogen atoms have been omitted for clarity.

trans-$Mo(DAniF)_2(O_2CCH_3)_2$ has two labile acetate groups *trans* to each other, there is also a possibility of obtaining a polymer with alternating bridging ligands and dimolybdenum units, but so far we have not been able to isolate such a compound. Conditions that may allow the isolation of higher oligomers or a polymer are being investigated. We are also investigating the possibility of coupling **4** and **5** in a ratio of 2:1 with the idea of creating a tetrad of dimolybdenum units.

Structural Results. Compound **1** crystallized in space group $P\bar{1}$ with the molecule residing on an inversion center. The core, depicted in Figure 2, shows that the two dimolybdenum units, each supported by three DAniF ligands, are linked by a fluoflavinate anion. The two Mo−Mo bonds are coplanar with the fluoflavinate anion, and the molecule

possesses idealized D_{2h} symmetry. While in compounds of this type with other linkers conformational variation occurs (for example, for dicarboxylate-linked complexes, a rotation about a C−C single bond is observed[10c] and in the β-diamidate-linked compounds, the dimetal-linker chelate ring is twisted.[14]), the molecules in **1** are conformationally rigid. This unique structural feature has an important impact on electronic communication between the two [Mo_2] units. The neutral molecule, **1**, has a typical quadruple-bond length, 2.0939(4) Å, for the two crystallographically equivalent dimolybdenum units. The two [Mo_2] units are separated by 7.174 Å, which is slightly greater than the 6.95 Å separation found in the oxalate analogue.[9a]

As shown by the ^{1}H NMR spectrum, the structure of **1** remains unchanged in solution. All signals for the supporting DAniF ligands are divided into two sets in a ratio of 2:1 for the ligands that are cis and trans to the fluoflavinate bridge. An example is that of the signals for the methine protons which appear at 8.33 and 8.65 ppm in a ratio of 2:1 in $CDCl_3$. The signals for the fluoflavinate anion appear at 5.69 and 3.52 ppm and show a significant upfield shift from the range (6−7.5) in which aromatic proton signals usually occur. This shift is caused by the high magnetic anisotropy of the dimolybdenum quadruple bond.[33] Since the protons on the fluoflavinate anion are located in the shielding cones of the magnetic anisotropy, the signals are displaced toward high field. It should also be noted that the downfield shift of the methine proton signals can also be attributed to the anisotropy of the Mo−Mo quadruple bond. The change in the direction of the shift is the result of the location of each group relative to that of the Mo_2^{4+} unit.[33]

The structures of two singly oxidized compounds have been determined. In **2a**, the counteranion is the symmetrical PF_6^- group. The cation in **2a** resides on a special position of monoclinic space group $C2/m$,[34] and the two [Mo_2] units are crystallographically equivalent. Because these crystals show considerable crystallographic disorder, crystals of the cation with the unsymmetrical trifluoromethanesulfonate (triflate) anion were also prepared, and this structure refined smoothly. The cation of **2b** (Figure 2) occupies a general position in the monoclinic space group $P2_1/n$ where the two Mo_2 units are crystallographically independent. The Mo−Mo bond distances for the two [Mo_2] units, 2.1084(8) Å and 2.1108(8) Å, are essentially the same, and they are longer than those in **1** by 0.015 Å, but they are significantly shorter than those found in compounds with similar coordination environments having units where the Mo_2^{5+} is localized on only one dimolybdenum unit.[12a,13] The similarity of the crystallographically independent Mo−Mo distances supports a symmetrical electronic structure where the unpaired electron is delocalized over both Mo_2 units via the bridging fluoflavinate anion.

(33) For example, see: Cotton, F. A.; Daniels, L. M.; Lei, P.; Murillo, C. A.; Wang, X. *Inorg. Chem.* **2001**, *40*, 2778 and references therein.

(34) Crystallographic data for **2a**·4CH_2Cl_2: space group $C2/m$, a = 18.432(3) Å, b = 23.183 (4) Å, c = 17.4429(3) Å, β = 121.227(3)°, V = 6368.8(1) Å^3, Z = 2, Mo−Mo distance =2.113(3) Å.

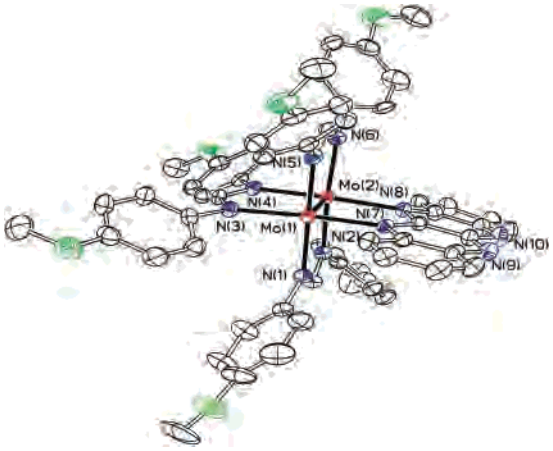

Figure 3. Core of **4** with displacement ellipsoids drawn at the 40% probability level.

The doubly oxidized compound **3** crystallized in triclinic space group $P\bar{1}$ with Z = 1. The dication (Figure 2) resides on an inversion center while the PF_6^- ions reside on general positions. The removal of two electrons from **1** to give **3** increases the Mo−Mo distances from 2.0939(4) to 2.1245(5) Å. The increase of 0.030 Å, is twice as large as that observed for the one-electron oxidation product **2b**. The magnitude of the change is also compatible with that observed in the β-oxamidate-linked analogues, where the lengthening of the Mo−Mo bond resulting from double oxidation is 0.04 Å.[14]

Even though the oxidation states for the Mo atoms in **1**, **2** (**a** and **b**), and **3** are different, the core structures of the three complexes are essentially the same. However, for the three compounds of the electron-transfer series, the average Mo−N_{DAniF} distances decrease from 2.155 to 2.141 to 2.124 Å as the charge increases on the dimetal units from 0 to 1 to 2. The variation of these metal−ligand distances, as well as the changes in the metal−metal distances, provides strong evidence that the first two of the three one-electron oxidation processes that appear on the CV correspond to metal-based oxidations.

Compound **4** crystallizes in monoclinic space group $P2_1/c$ with Z = 4. The core structure, shown in Figure 3, consists of a quadruply bonded dimolybdenum unit bridged by three DAniF groups and a monoanionic fluoflavinate anion. The metal−metal bond distance, 2.0931(3) Å, is similar to that in **1**. The molecule has idealized C_{2v} symmetry. This symmetry does not change in solution, as shown by its ^{1}H NMR spectrum. There are four groups of signals of the same intensity assigned to the fluoflavinate protons. The signals are scattered in a wide range from 6.56 to 3.62 ppm because of the variable influences of the magnetic anisotropy of the Mo−Mo quadruple bond.

The core structure of **5** is shown in Figure 4, and the structural parameters are listed in Table 2. This compound has the same fluoflavinate linker as **1**, but it has slightly different metal subunits. Each dimolybdenum unit is supported by two DAniF units cis to the fluoflavinate and an acetate group that is trans. The molecule crystallizes in the space group of $P\bar{1}$ with Z = 1. The bond distances are very

Table 3. Influence of Linker, L, on $\Delta E_{1/2}$ and K_C in Some $[Mo_2]L[Mo_2]$ Species

linker	relative orientation of $[Mo_2]$ units	$[Mo_2]\cdots[Mo_2]$ (Å)	$E_{1/2}^{+/0}$ (mV)	$E_{1/2}^{2+/+}$ (mV)	$\Delta E_{1/2}$ (mV)	K_c	ref
fluoflavinate (in **1**)	∥	7.174	79	495	416	1.1×10^7	this work
fluoflavinate (in **5**)	∥	7.108	199	619	420	1.3×10^7	this work
α-diphenyloxamidate	⊥	7.096	176	367	191	1.7×10^3	16
α-di-*p*-anisyloxamidate	⊥	7.081	183	373	190	1.6×10^3	16
oxalate	∥	6.953	294	506	212	3.8×10^3	9b

similar to those of **1**. In the ^{1}H NMR spectrum of **5**, signals from the fluoflavinate protons are shifted to high field, just as they are in **1**, because of the anisotropy of the Mo_2 quadruple bond. With a labile acetate group on each end, compound **5** has the potential to be used to construct an equatorially linked dimolybdenum chain spaced by conjugated fluoflavinate groups.

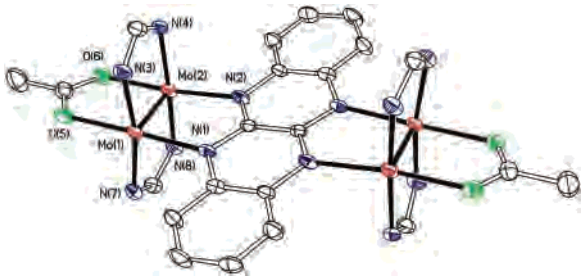

Figure 4. Core of **5** in $5{\cdot}4CH_2Cl_2$ with displacement ellipsoids drawn at the 40% probability level. All *p*-anisyl groups and hydrogen atoms have been omitted for clarity.

Electrochemistry. The prominent electrochemical feature for **1** is the existence of three reversible one-electron waves (Figure 1). Compound **5** also shows three reversible redox couples at 199, 619, and 1004 mV (Table 3). As mentioned earlier, the structural data support the assignment of the first two waves as being metal-based oxidations, but they offer no clues for the assignment of the third one, at the highest potential. Since no compound could be isolated from our attempts to prepare a triply oxidized species, the electrochemistry of the paddlewheel compound $Mo_2(DAniF)_3(HC_{14}H_8N)$, **4**, was studied. Compound **4** shows two reversible one-electron oxidation processes at 390 and 795 mV. These potentials are much lower than those in **1**. The appearance of two redox processes is rather unusual in dimolybdenum systems, and very few examples of this are known.[35] Calculations at the DFT level (vide infra) suggest that the redox process at 795 mV is associated with the fluoflavinate linker which is noninnocent under the electrochemical conditions of the experiment. By comparison, the third redox process in **1** may be assigned to the fluoflavinate anion. In the radical cation, the additional unpaired electron is expected to reside in a ligand-based orbital. This assignment is also consistent with the high instability of the triply oxidized product of **1**.

Attempts to conduct electrochemical measurements on fluoflavine itself were unrewarding because of its very low solubility in organic solvents. To circumvent this problem, we have made the 2-methyl derivative, which has enough solubility to allow measurement of its electrochemistry. It shows a redox process at $E_{1/2} = 920$ mV. This value is between the high potential in **4** (795 mV) and that for **1** (941 mV), and it has been assigned to the oxidation of the amine.[36]

Following the preceding assignment of the redox potentials to the corresponding redox sites, one can evaluate the degree of the electronic communication in MV species **2**. The CV and DPV of **1** show that the oxidation potentials for the two $[Mo_2]$ units are separated by 416 mV or $\Delta E_{1/2}(1) = E_{1/2}^{(2+/1+)} - E_{1/2}^{(1+/0)}$. From this value of $\Delta E_{1/2}$, a comproportionation constant (K_C) of 1.1×10^7 can be derived.[37] This magnitude of K_C indicates that the two $[Mo_2]$ units in **1** are strongly electronically coupled by the fluoflavinate linker and the mixed-valence species, **2a** and **2b**, are thermodynamically stable with respect to the neutral compound **1** and doubly oxidized compound **3**. The large K_C value (1.1×10^7) is similar to those in the β-isomers of the oxamidate analogue in which the K_C is 9.5×10^8.[14] These oxamidate analogues have been classified as Class III because of the large electron delocalization.

In contrast, in the α-oxamidate linked compound which has two orthogonal $[Mo_2]$ units, the possibility of metal−ligand orbital overlap is eliminated, and the mixed-valence species has been spectroscopically and structurally characterized to be electron localized, Class I.[16] For the oxalate anion linked compound, whose conformation may change as a rotation about the C−C single bond takes place, only weak coupling between the two $[Mo_2]$ units is observed. Although the metal−metal separations in all compounds in Table 3 are similar, for the fluoflavinate compounds there is an increase of over 200 mV in ΔE. It should also be noted that the potentials in **5** are shifted to higher values relative to those in **1**, in keeping with the lower basicity of the acetate bridge, but the $\Delta E_{1/2}$ values are similar.

It is clear that the fluoflavinate linker plays a critical role in enhancing the electronic communication, and this is the result of the rigid conjugated π system of the anion and the robust structure of the molecule. The rigidity and planar conformation of the linker allow continuous orbital overlap to be established between the metal δ orbitals and the linker π orbitals. Thus, the linker in the doubly oxidized **3** can be

(35) For example, see: Cotton, F. A. In *Multiple Bonds between Metal Atoms*, 3rd ed.; Cotton, F. A., Murillo, C. A., Walton, R. A., Eds.; Springer Science and Business Media, Inc.: New York, 2005; Chapter 4.

(36) Electrochemical oxidation of aromatic amines has been a widely studied phenomenon. Often dimerization of two radical cations is observed before deprotonation. For example, see: (a) Larumbe, D.; Moreno, M.; Gallardo, I.; Bertrán, J.; Andrieux, C. P. *J. Chem. Soc., Perkin Trans. 2* **1991**, 1437. (b) Awano, H.; Murakami, H.; Yamashita, T.; Ohigashi, H.; Ogata, T. *Synth. Met.* **1991**, *39*, 327.

(37) Richardson, D. E.; Taube, H. *Inorg. Chem.* **1981**, *20*, 1278.

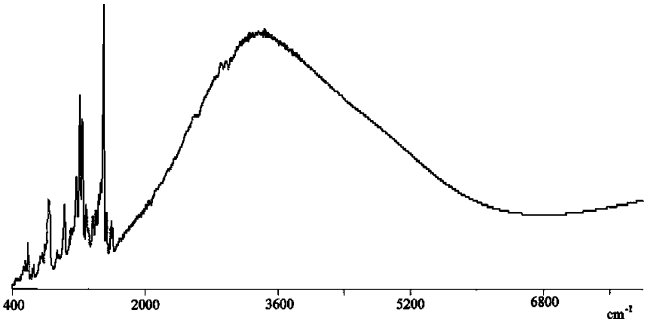

Figure 5. Near-IR spectrum of the mixed-valence species **2a** using a KBr pellet.

thought of as a tetraazatetracene which is analogous to the well-known aromatic tetracene, often called naphthacene.[38]

Near-IR Spectrum. The spectrum of a solid sample of **2a** in a KBr pellet, measured in the 1600−6000 cm^{-1} region, shows a relatively intense band, somewhat unsymmetric, peaking at about 3400 cm^{-1} and centered at about 3800 cm^{-1} (Figure 5). The observed bandwidth, $\Delta\nu_{1/2}$, of about 2100 cm^{-1} is significantly smaller than the 2820 cm^{-1} value calculated using the Hush formula, $\Delta\nu_{1/2} = (2310\ \nu_{max})^{1/2}$ cm^{-1}.[4b,39] Since the value from the Hush model is the prediction for a Class II compound, a narrower band is generally considered to be an indication that the electronic communication is better than that in a Class II compound. This band is similar to that in the $\{[Bu^tCO_2)_3Mo_2]_2(\mu$-oxalate$)\}^+$ ion.[40] Thus, the near-IR spectrum is consistent with structural results, suggesting that the fluoflavinate linker mediates strong electronic coupling between the two linked $[Mo_2]$ units, and resembles the previously reported Class III β-oxamidate-bridged analogues.[14]

EPR Spectrum and Magnetism. The X-band electron paramagnetic resonance spectrum of the singly oxidized **2a** in frozen CH_2Cl_2 solution exhibits a symmetric signal devoid of hyperfine structure. The g_{iso} value of 1.943 is significantly lower than that for a free organic radical, indicating that the odd electron resides in a metal-based orbital.[13,41] Such an assignment is also consistent with the structural data discussed before. In the absence of observed hyperfine structure, the EPR spectrum provides no evidence concerning the extent of delocalization of the unpaired electron.

Magnetic susceptibility measurements on a crystalline sample of **2a**, from 5 to 300 K, show that χT in this temperature range has an essentially constant value of ca. 0.38 emu K mol^{-1}. This value is within the range expected for a system with one unpaired electron and is consistent with the EPR spectrum and crystal structure of the singly oxidized species.

The magnetism for compound **3**, measured in the same temperature range (5 to 300 K), shows a small residual χT value. The value changed from sample to sample, but it was always temperature independent for any one sample. This is consistent with the presence of a compound that is essentially diamagnetic but always contaminated with a small, but variable, amount of the singly oxidized species **2**. The source of **2** is not certain but presumably it is produced because of the instability, already mentioned, of **3**. The diamagnetism is consistent with strong electronic coupling between the $[Mo_2]$ units, as observed in the β-oxamidate system, which gives a singlet ground state.[14]

DFT Calculations and Electronic Structure. On the basis of symmetry considerations, a qualitative description of the bonding and MO interactions that develop between the frontier $[Mo_2]$ δ orbitals and the π orbitals of the fluoflavinate linker can be obtained, as shown in Figure 6. On the right of the figure are the two highest-occupied $[Mo_2]$-based orbitals which are composed of the in-phase (b_{1u}) and out-of-phase (b_{2g}) combinations of the δ orbitals, $\delta + \delta$ and $\delta - \delta$, respectively, and two unoccupied $[Mo_2]$-based orbitals composed of in-phase (b_{3g}) and out-of-phase (a_u) combinations of the δ^* orbitals, $\delta^* + \delta^*$ and $\delta^* - \delta^*$, respectively. On the left side of the diagram are orbitals that come from the ligand π system. The two highest-occupied orbitals of the ligand have b_{2g} and b_{3g} symmetries, and the three lowest unoccupied orbitals have b_{1u}, b_{3g}, and a_u symmetries. By combining the ligand- and metal-based orbitals, we obtained the MO diagram in the central section of Figure 6. The metal-based b_{2g} orbital is higher in energy because of the interaction with the filled b_{2g} ligand orbital, whereas the metal-based b_{1u} orbital is stabilized because of a back-bonding interaction with the empty b_{1u} ligand orbital. In this diagram the occupied b_{3g} ligand orbital is placed at higher energy than the metal-based b_{1u} orbital to be consistent with the experimental observation of a third reversible redox process that has been assigned as being a ligand-based oxidation.

This qualitative picture is useful for the interpretation of the electronic structures of **1**, **2**, **3**, and the paddlewheel species, **4**, which were investigated with density functional theory. For practical reasons, simplified models in which each of the *p*-anisyl groups of the formamidinate ligands was replaced by a hydrogen atom were utilized for all the calculations.[42] For comparison purposes, three different functionals (B3LYP, mPW1PW91, and BP86) were utilized in this work, and the calculated distances for all models are shown in Table 4.

Geometry optimization results for the models of **1**, **2**, and **3** show that the bond distances calculated using the mPW1PW91 functional are in close agreement with the experimental results obtained by X-ray crystallography. For example, the calculated Mo−Mo bond distances for the model of **1** are only 0.02 Å longer than the experimental distances, whereas the calculations with B3LYP and BP86 overestimate this distance by 0.04 and 0.06 Å, respectively. The mPW1PW91 functional also provides better accuracy than B3LYP and BP86 when the Mo−N bond distances are calculated.

(38) For example, see: Moon, H.; Zeis, R.; Borkent, E.-J.; Besnard, C.; Lovinger, A. J.; Siegrist, T.; Kloc, C.; Bao, Z. *J. Am. Chem. Soc.* **2004**, *126*, 15322.
(39) Hush, N. S. *Coord. Chem. Rev.* **1985**, *64*, 135.
(40) Chisholm, M. H.; Pate, B. D.; Wilson, P. J.; Zalesky, J. M. *Chem. Commun.* **2002**, 1084.
(41) (a) Cotton, F. A.; Pederson, E. *Inorg. Chem.* **1975**, *14*, 399. (b) Cotton, F. A.; Daniels, L. M.; Hillard, E. A.; Murillo, C. A. *Inorg. Chem.* **2002**, *41*, 1639.
(42) Previous studies on similar systems have shown that such simplification is reasonable. For example, see ref 14.

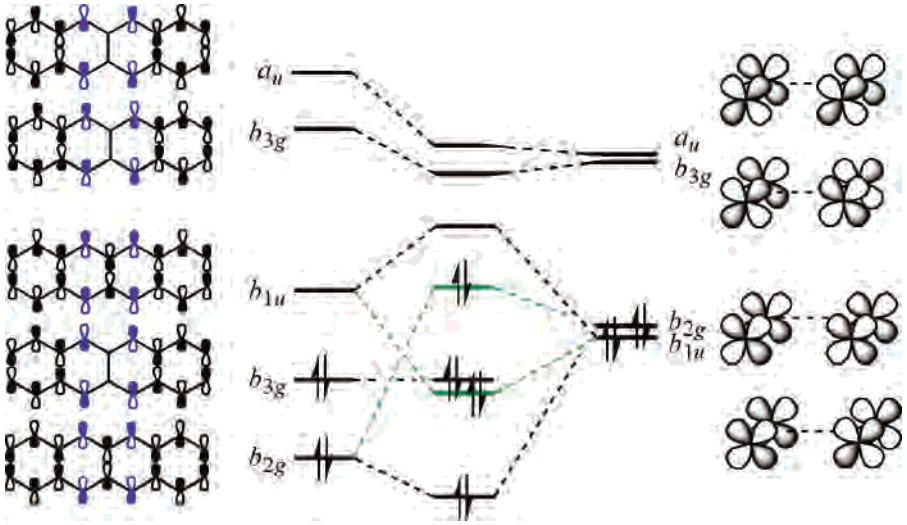

Figure 6. Frontier orbital interactions between the δ orbital combinations of the [Mo_2] units and π orbitals of the fluoflavinate linker. In the left column, the nitrogen p orbitals of the fluoflavinate are shown in blue. In the center, the metal δ-based orbitals are shown in green.

Table 4. Calculated Distances for the Models of **1**, **2**, and **3**

				selected distances (Å)			
functional	model	charge	spin	Mo−Mo	C−C[a]	Mo−N[b]	$Mo_2\cdots Mo_2$
B3LYP	**1**	0	0	2.1322	1.4587	2.1804	7.2193
	2	1	1/2	2.1482	1.4475	2.1492	7.1529
	3	2	0	2.1579	1.4427	2.2198	7.1845
		2	1	2.1630	1.4682	2.1797	7.2034
mPW1PW91	**1**	0	0	2.1158	1.4513	2.1576	7.1595
	2	1	1/2	2.1333	1.4393	2.1268	7.0942
	3	2	0	2.1488	1.4273	2.0998	7.0390
		2	1	2.1467	1.4616	2.1594	7.1471
BP86	**1**	0	0	2.1554	1.4573	2.1711	7.2235
	2	1	1/2	2.1682	1.4525	2.1518	7.1782
	3	2	0	2.1742	1.4500	2.2273	7.2258
		2	1	2.1784	1.4672	2.1622	7.2414
experimental	**1**	0	0	2.0939	1.450	2.163	7.174
	2	1	1/2	2.1084[b]	1.429	2.128	7.100
	3	2	0	2.1245	1.427	2.130	7.090

[a] The central C−C bond in the fluoflavinate linker. [b] Average values for two dimetal units.

A similar result is obtained in the calculation of the distances in the model of the singly oxidized compound **2**. Again the mPW1PW91 functional gives the best agreement with the X-ray structural parameters. However, all three functionals were capable of reproducing the magnitude of the experimental increase in Mo−Mo distances (0.015 Å) compared to those observed in their respective neutral models. This increase is consistent with the effect of removing an electron from a bonding metal δ orbital and leaving a positive charge delocalized over two [Mo_2] units.

Although the experimental data favor a singlet spin state for the doubly oxidized compound **3**, calculations were done on models in two possible spin states, $S = 0$ and $S = 1$. For each spin state, calculations were performed with each of the three functionals mentioned above. In general, the calculated distances from the singlet state calculations are in better agreement with the crystallographic values than those obtained from the triplet state calculations. For instance, the calculated Mo−Mo bond distances for the singlet state for each functional, although generally overestimated, are shorter than those from the triplet state calculations. To summarize, for all calculated models of different oxidation states, mPW1PW91 consistently provided significantly better structural parameters than B3LYP, and BP86 typically yielded results that differ the most from the experimental values.

Graphic illustrations of the frontier B3LYP MOs of the model of **1** are shown in Figure 7, and energy results for all calculated models are in Table 5. As anticipated from the qualitative depiction in Figure 6, regardless of the functional utilized, the HOMO consists of the out-of-phase combination of δ orbitals of b_{2g} symmetry with some contribution from the b_{2g} ligand orbital.[43] Also, as expected, the HOMO-1 and HOMO-2 are calculated to be very close in energy (0.09 eV according to the B3LYP calculation). For the three functionals, the HOMO-1 is always the in-phase combination of the δ orbital with a significant contribution of the b_{1u} ligand orbital,[44] and the HOMO-2 is the ligand-based b_{3g}. For the model of **2**, the electronic structure is similar to that for the model of **1**. The SOMO is composed of the metal-based b_{2g} orbital, $\delta - \delta$. This is consistent with the EPR spectrum that shows a low value of g (1.94), which indicates that the unpaired electron is distributed over a mainly metal-based MO.

The electronic structure of the model of the doubly oxidized singlet state may be derived from that of the neutral molecule by removal of the b_{2g} electrons (see Figures 6 and 7). For all functionals used in the calculations, the HOMO is the metal-based b_{1u} orbital ($\delta + \delta$) and the HOMO-1 is the ligand based b_{3g}, while the LUMO is the metal-based b_{2g} ($\delta - \delta$), which is occupied in the neutral and singly oxidized models. In the triplet state, $S = 1$, the b_{2g} and b_{1u} metal-based orbitals are both singly occupied.

It should be noted that the bond distances of the singlet state are in better agreement with the experimental results

(43) The relative composition of the HOMO with respect to metal and bridge ligand character is 73, 72, and 72% metal and 7, 8, and 5% bridge according to B3LYP, mPW1PW91, and BP86, respectively.

(44) The relative composition of the HOMO-1 with respect to metal and bridge ligand character is 69% metal and 13% bridge according to both B3LYP and mPW1PW91 and 66% metal and 12% bridge according to BP86.

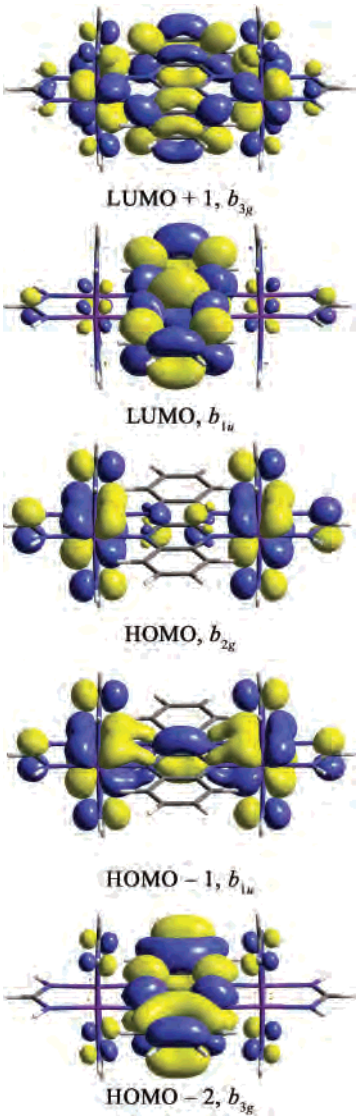

Figure 7. The 0.02 surface contour diagrams for the frontier molecular orbitals for the model of compound **1** calculated by DFT.

Table 5. Calculated Energies for the Models of **1**, **2**, **3**, and **4**

				energy (au)		
model	charge	multiplicity	spin	B3LYP	mPW1PW91	BP86
1	0	1	0	−1924.1702	−1923.8475	−1924.6304
2	+1	2	1/2	−1923.9991	−1923.6760	−1924.4586
3	+2	1	0	−1923.7035	−1923.3749	−1924.1680
3	+2	3	1	−1923.7175	−1923.3960	−1924.1631
3	+2	1	BS	−1923.7196	NA	NA
4	0	1	0	−1341.2982	−1341.0520	NA

than those from the triplet state. However, the total energy of the triplet state calculated with both hybrid functionals was lower than that of the singlet state (0.38 and 0.57 eV for B3LYP and mPW1PW91, respectively) and only slightly higher (0.13 eV) for BP86. Because the amount of Hartree−Fock exchange in hybrid functionals B3LYP and mPW1PW91 tends to favor higher multiplicity states, the energy difference between the singlet and triplet states is likely to be underestimated. Previous work[14] on compounds of the type $[Mo_2]L[Mo_2]$ has also shown that the broken-symmetry (BS) method[45] is useful for modeling partially delocalized systems utilizing unrestricted DFT and that this approach can be coupled with Yamaguchi's relationship[46,47] to compute an accurate estimate[48] of the Heisenberg magnetic exchange coupling constant, $2J$. As shown in Table 5, the application of the BS approach[49] indeed provides a lower energy than the triplet state, and the use of Yamaguchi's relationship gives an estimated $2J$ value of -923 cm^{-1},[50] which is consistent with the magnetic susceptibility results that show that **3** is a diamagnetic system at and below 300 K.

It is also worth noting that for the singlet state of the doubly oxidized model of **3**, the calculated energy difference between the HOMO, b_{1u}, and HOMO-1, b_{3g}, is very small. Thus, it is possible that, in solution, the ligand-based b_{3g} orbital may be the HOMO, and this may account for the third oxidation wave observed in the cyclic voltammogram. Similarly, the electronic structure of a model of paddlewheel compound **4**, obtained with B3LYP, shows that, while the HOMO is primarily metal δ, the HOMO-1 is ligand based. This supports the assignment of the second oxidation wave in **4** as being ligand-based and suggests that the assignment of the third wave in the CV of **1** to a ligand redox process is correct.

Finally, TD-DFT calculations were also performed on all three models of **1** and **2** to help assign the lowest-energy transitions in their UV−vis electronic spectra and the NIR of **2**. The results indicate that for **1** the band at 512 nm may be assigned to a $\delta - \delta \rightarrow \pi$-ligand (HOMO → LUMO) transition, which is allowed in x polarization and calculated at 534 nm. The band at 482 nm may be assigned to a $\delta + \delta \rightarrow \delta^* + \delta^*$ transition, allowed in y polarization, and calculated at 490 nm. The band at 460 nm may be assigned to a $\delta - \delta \rightarrow \delta^* - \delta^*$ transition, calculated at 472 nm and which is also allowed in y polarization. For **2**, the intense NIR band at 3800 cm^{-1} is mainly a $\delta - \delta \rightarrow \delta + \delta$ (HOMO-1 → SOMO) transition calculated at 5618 cm^{-1} ($f = 0.168$). This is the so-called *intervalence* band that is typically observed for compounds near the Class II/Class III border. The bands observed in the visible region for **2** at 622 and 550 nm may be assigned to the $\delta + \delta \rightarrow \delta^* + \delta^*$ and $\delta - \delta \rightarrow \delta^* - \delta^*$ transitions, and they are calculated at 815 and 578 nm, respectively.

(45) (a) Noodleman, L. J. *Chem. Phys.* **1981**, *74*, 5737. (b) Noodleman, L.; Baerends, E. J. *J. Am. Chem. Soc*. **1984**, *106*, 2316. (c) Noodleman, L.; Davidson, E. R. *Chem. Phys.* **1986**, *109*, 131. (d) Noodleman, L.; Peng, C. Y.; Case, D. A.; Mouesca, J.-M. *Coord. Chem. Rev.* **1995**, *144*, 199.
(46) Soda, T.; Kitagawa, Y.; Onishi, T.; Takano, Y.; Shigeta, Y.; Nagao, H.; Yoshioka, Y.; Yamaguchi, K. *Chem. Phys. Lett*. **2000**, *319*, 223.
(47) The magnetic exchange coupling constant, $2J$, is based on the Heisenberg−Dirac−VanVleck spin Hamiltonian $H = -2JS_1S_2$. *Yamaguchi's relationship is provided by the following equation:* $J = E^{BS} - E^{HS}/\langle S^2\rangle^{HS} - \langle S^2\rangle^{BS}$ (see ref 46), where E^{BS} and E^{HS} represent the total energy values of the broken-symmetry and high-spin DFT calculations, respectively.
(48) Kiehl, P.; Rohmer, M.-M.; Bénard, M. *Inorg. Chem.* **2004**, *43*, 3151.
(49) The B3LYP functional was used for studies involving the BS approach because this functional has a smaller energy overestimation compared to that of the hybrid functional mPW1PW91. For BP86, the broken-symmetry method did not lower the energy.
(50) The calculated $\langle S^2\rangle^{BS}$ and $\langle S^2\rangle^{HS}$ values are 1.00 and 2.04, respectively, and the E^{BS} and E^{HS} values are given in Table 5.

Concluding Remarks

The large rigid conjugated fluoflavinate anion is the first all-nitrogen donor ligand that has been used to link dimetal units to form dimer-of-dimers type compounds. The electrochemistry of this compound shows three one-electron redox couples: two have been assigned to metal-based oxidations and the third one to a ligand-based oxidation. All three members of the electron-transfer series, $[Mo_2]$fluoflavinate$[Mo_2]^{n+}$ (n = 0, 1, and 2), were structurally characterized. Various spectroscopic techniques and DFT calculations indicate that the fluoflavinate dianion is a strong mediator of electronic communication. This complex system provides an excellent example of how intramolecular electron transfer can be modified by ligand design.

Calculations at the DFT level were carried out using three functionals, B3LYP, mPW1PW91, and BP86, to study the electronic structures of **1**, **2**, **3**, and **4** with the idea of evaluating how well the calculated results reproduce experimental data in $[Mo_2]L[Mo_2]$ compounds. The frontier orbitals of such systems consist of in-phase and out-of-phase combinations of the δ orbitals mediated by the bridge ligand. The results obtained by the three functionals are qualitatively consistent with each other, and the calculations using mPW1PW91 yield geometries of remarkable accuracy compared to the crystal structures obtained by X-ray diffraction.

Acknowledgment. We thank the National Science Foundation, the Robert A. Welch Foundation, and Texas A&M University for financial support. We also thank the Laboratory for Molecular Simulation for hardware and software and the Texas A&M University supercomputer facility. We are grateful to Dr. Lisa M. Pérez for helpful discussions.

Supporting Information Available: X-ray crystallographic files in CIF format for **1**·$4CH_2Cl_2$, **2b**·$7.5CH_2Cl_2$, **3**·$4CH_2Cl_2$, **4** and **5**·$4CH_2Cl_2$. This material is available free of charge via the Internet at http://pubs.acs.org.

IC051614D